ENVIRONMENTAL RESEARCH
LETTERS

LETTER • OPEN ACCESS

Causes on the 2018 record-breaking heatwave in South Korea: compound impacts from recurrent large-scale atmospheric teleconnections

To cite this article: Hyerin Kim *et al* 2024 *Environ. Res. Lett.* **19** 124064

ENVIRONMENTAL RESEARCH
LETTERS

CrossMark

OPEN ACCESS

RECEIVED
16 June 2024

REVISED
11 September 2024

ACCEPTED FOR PUBLICATION
24 September 2024

PUBLISHED
19 November 2024

LETTER

Causes on the 2018 record-breaking heatwave in South Korea: compound impacts from recurrent large-scale atmospheric teleconnections

Hyerin Kim[1,5], Nakbin Choi[2,3,5], Myong-In Lee[1,2,*], Sunlae Tak[2], Dong-Hyun Cha[1,2] and Seung-Ki Min[4]

[1] Graduate School of Carbon Neutrality, Ulsan National Institute of Science and Technology, Ulsan, Republic of Korea
[2] Department of Civil, Urban, Earth, and Environmental Engineering, Ulsan National Institute of Science and Technology, Ulsan, Republic of Korea
[3] Department of Atmospheric, Oceanic and Earth Sciences, George Mason University, Fairfax, VA, United States of America
[4] Division of Environmental Science and Engineering, Pohang University of Science and Technology, Pohang, Republic of Korea
[5] Co-first authors equally contributed to this work.
[*] Author to whom any correspondence should be addressed.

E-mail: milee@unist.ac.kr and khrmirror@unist.ac.kr

Keywords: heatwave, Pacific–Japan (PJ), circum-global teleconnection (CGT), Arctic Oscillation (AO) pattern, atmospheric pattern

Supplementary material for this article is available online

Abstract

This study analyzed the causes of the extreme heatwave in East Asia in 2018, which brought a record-breaking event in South Korea in terms of the number of hot days and the intensity in history. Long-lasting atmospheric patterns were observed during the 2018 heatwave, and the patterns were similar to those known as the Pacific–Japan (PJ), circum-global teleconnection (CGT), and Arctic Oscillation (AO) patterns identified in a previous study. In 2018, all three patterns appeared to exhibit a strong positive phase. In particular, the PJ and AO Indices showed the highest values within the analysis period, having a major impact on the heatwave. According to a quantitative analysis through multi-linear regression (MLR) of how much each of the three patterns affects the heatwave, all three patterns of PJ, CGT, and AO have significant effects on the heatwave in Korea. The statistically reconstructed heatwave days (HWD) time series with the three indices by MLR account for 51% of the total variability at the interannual timescale. Especially in 2018, most of the occurred HWD could be restored using the three indices. Also, in 1994, when the three indices had a high peak, the number of HWDs was the second-longest ever, while in 1993, when all three indices had a low peak, the heatwave was the lowest. This study quantitatively examined whether the large-scale extreme heatwave in 2018 greatly increased because of PJ, CGT, and AO. This study suggests that extreme heatwave can occur again if three apparently independent atmospheric patterns appear at once in the future.

1. Introduction

The heatwave frequency on the Korean Peninsula has increased over the past 45 years despite regional differences in trends (Choi and Lee 2019). In particular, the 2018 heatwave was the most powerful case in the history of observations in Korea in terms of its scale and damage. According to the statistics of the Korea Meteorological Administration (KMA), the heatwave incidents recorded 31.0 d on average over the entire 62 observation stations for the whole year, breaking the record of 29.6 d in 1994, the highest record before the record high in 2018. In the case of the heatwave duration, the highest record was 36 d in Gwangju. On 1 August, the highest daily temperature in Hongcheon was 41 °C, and the lowest daily temperature in Seoul was 30.3 °C on 2 August. This record-breaking heatwave continued from mid-July to mid-August. According to the previous study, 929 deaths were recorded and caused by the extreme heatwave in 2018 (Park and Chae 2020). The number of patients with thermal diseases was up to four times higher than the average for the last four years (Ha *et al* 2020). However, by what mechanisms such an unprecedented heatwave event in 2018 was manifested has not been fully explained, although Ha *et al* (2020) presented the importance of blocking patterns, and Ren *et al* (2020) investigated the contribution of atmospheric circulation changes. Previous studies have not clearly suggested the root cause of such a persistent upper-level high-pressure system in East Asia.

Although the increase in background temperature due to global warming cannot be neglected in increasing the probability of heatwave occurrence (Pachauri *et al* 2014, Min *et al* 2015, 2020, Kim *et al* 2018), the number of heatwave days (HWDs) on the Korean Peninsula exhibits substantial year-to-year variation, suggesting various dynamical mechanisms (Yeo *et al* 2019). Previous studies have suggested mechanisms related to the manifestation of upper-level large-scale circulation anomalies maintained at the sub-seasonal to seasonal timescale. Once the upper-level high-pressure anomalies associated with large-scale teleconnection and stationary waves are sustained for a long time, they can lead to a more intense heatwave due to an increase in ambient temperature caused by global warming. Min *et al* (2020) suggested the important role of the background temperature increase in intensifying the 2018 summer heatwave in South Korea, which accompanied the stationary wave formation triggered by convection in Northwest India and the Southern China Sea.

Geographically Northeast Asia, including the Korean Peninsula, is located at the mid-latitude and the border of the continent and the ocean, and it can be affected by various climate variabilities originating from tropical oceans, mid-latitude continents, and the Arctic. Several studies have attempted to analyze the causes of heatwave in the Korean Peninsula. Park and Schubert (1997) examined that the Western North Pacific (WNP) High, which developed earlier than normal in 1994 influenced the occurrence of the heatwave, in addition to the upper-level atmospheric circulation associated with the Pacific–Japan teleconnection (PJ; Nitta 1988) initiated by tropical convection. Lee and Lee (2016) analyzed the upper-level atmospheric circulation patterns responsible for the interannual variability of the Korean Peninsula heatwave. They identified two remote impacts from the Arctic Oscillation (AO; Thompson and Wallace 1998) and the PJ from the tropics.

On the other hand, Kim *et al* (2018) suggested that heatwave occurring on the Korean Peninsula in July–August are related to summer precipitation and convective variability in regions from northeast Pakistan to northwest India, based on data analysis for the last 42 years. This convection variability guides the teleconnection pattern manifested with mid-latitude stationary wave trains with zonal wavenumbers 5–6, known as the circum-global teleconnection (CGT; Ding and Wang 2005). Choi *et al* (2020) analyzed the mechanisms of heatwave in East Asia, including the Korean Peninsula, in terms of large-scale teleconnections and their decadal changes. Compared to the active CGT pattern in the past, the Scandinavia teleconnection pattern has become as important as the CGT in recent years, suggesting that land-atmosphere coupling has been strengthened in the Eurasian continent in recent years.

Previous studies revealed that high-pressure anomalies in the upper levels of the Korean Peninsula were the leading cause of long-lasting heatwave, and these anomalous circulations can be developed by various teleconnection mechanisms from the tropics, mid-latitudes, and the Arctic. However, there is insufficient research on which is dominant. This is the main motivation for this study to be addressed based on a long-term observational analysis of the large-scale circulation patterns. This study also attempts to verify the hypothesis that a stronger heatwave can be maintained when several teleconnection patterns develop jointly. Building on the previous studies, this study mainly focuses on the changes in three large-scale teleconnection patterns indicated as the most dominant mechanisms for the Korean heatwave: CGT, PJ, and AO. This study investigates the long-term variations in the occurrence frequency of heatwaves on the Korean Peninsula and associates them with three teleconnection variations. This analysis can explain which teleconnection is mainly responsible for heatwaves in a specific year and whether two or three teleconnection patterns occur together and provide combined impacts. Specifically, this study explores the dynamic mechanisms most responsible for the record-breaking 2018 heatwave.

Section 2 of this paper describes the observational data and reanalysis data used in this study and the analysis method. In section 3, the large-scale patterns of the Korean Peninsula heatwave in 2018 are presented and explained using dynamic teleconnection mechanisms. Finally, section 4 provides a summary and conclusions.

2. Data and methodology

2.1. Data

Daily maximum temperature data were obtained from the 45 Automated Synoptic Observing System (ASOS) stations of the KMA. The National Centers for Environmental Prediction /National Center for Atmospheric Research Reanalysis 1 (Kalnay *et al* 1996) was used to analyze the large-scale atmospheric circulation patterns for 1979–2023. The dataset has a 2.5° × 2.5° (latitude × longitude) horizontal resolution with 17 vertical levels, and is available daily and monthly. Geopotential height at 200 hPa, 500 hPa, and 850 hPa, u-wind, v-wind, and sea level pressure

(SLP) were used to calculate the teleconnection pattern indices and analyze the atmospheric state in the summer of 2018.

2.2. Methodology

This study examined the data in high summer (July–August), the peak season for heatwaves in South Korea after the seasonal East Asian monsoon rainfall period (Lee and Lee 2016). This study first constructed a time series of HWDs for 45 years with the sum of averaged hot days when the daily maximum temperature exceeds 33 °C over 45 ASOS stations for July–August.

The PJ pattern was obtained from the first mode of the Empirical Orthogonal Function (EOF) analysis to the monthly-mean 850 hPa vorticity fields over the WNP (10°–55° N, 100°–160° E) after applying a T21 triangular truncation (approximately 5° × 5°) spatial filter (Kosaka and Nakamura 2010) for horizontal smoothing. The PJ index was defined as the principal component time series associated with the PJ mode. The CGT index was calculated by a regional mean of 200 hPa GPH monthly anomalies for northwest India (35°–40° N, 60°–70° E), following the definition by Ding and Wang (2005). The AO index was obtained from the principal component time series of the first EOF mode of monthly-mean SLP on the north of 20°N (Thompson and Wallace 1998). No time filter was applied to the indices to retain their value in 2018.

Multiple linear regression (MLR) was used to examine the quantitative contribution from the three teleconnection modes, with the predictand of HWD and the three predictors of PJ, CGT, and AO indices. A linear trend was considered separately in MLR. Each predictor was almost independent with weak correlations (table 1), so that individual contribution was represented quantitatively with the coefficient of each predictor. MLR is the least-squares approximation by minimizing the sum of squared differences between the predictand i.e. HWDs and the MLR-predicted values. All statistical significance tests were based on the Students' t-test at 1% and 5% significance levels. This study conducted the leave-one-out cross-validation for the MLR analysis (Wilks 2011). This was done by comparing the actual observed values with the predicted values for each year, which were obtained by fitting an MLR model using data from all other years except the year being predicted.

This study also performed the lower-tropospheric and surface energy budget analysis during the 2018 heatwave period. The vertically-averaged temperature equation for 1000–850 hPa is represented as:

$$\frac{\partial T}{\partial t} = -V \cdot \nabla T + \omega\sigma + \frac{Q}{C_p} \tag{1}$$

where T is temperature, t is time, V is horizontal velocity, ∇ is horizontal gradient, σ is static stability defined as $\sigma = \frac{\mathrm{d}T}{\mathrm{d}p} - \frac{RT}{C_p P}$ with the gas constant R, pressure p, and the specific heat C_p. Therefore, the temperature tendency is balanced with the horizontal advection, vertical motion combining advection and adiabatic heating, and diabatic heating.

3. Results

3.1. Overview of the Korean heatwave in 2018

The number of HWDs in 2018 has been record-breaking since 1973 when the nationwide ASOSs observation began. The top-ranked event before 2018 is 1994. This extreme record in 2018 is strongly abnormal compared to the historical distribution of HWDs, and it corresponds to a 101 year return period based on a generalized extreme value (GEV) distribution fit (supplementary figure 1). According to figure 1(a), the heatwave lasts during high summer (July–August). During this period, the termination of the summer monsoon (Changma) occurs on 11 July, which is much earlier than the climatology on 26 July. Because of this early cessation of the rainfall period and the northward expansion of the WNP high system, the temperature increases in early July, and hot weather continues until mid-August in 2018.

During high summer, heatwaves occurred 29.8 d in 2018 and 28.8 d in 1994 on average (figure 3). Although these two years show comparable values for HWDs, the intensity of the heatwave is much stronger in 2018. Figure 1(b) shows the maximum values of the daily maximum temperature from July to August 2018. When comparing to the 1994 case, more than half of the observation stations recorded extremely high temperatures exceeding 38 °C in 2018, whereas it was less than half in 1994 (supplementary figure 2). In particular, no stations recorded temperatures exceeding 40 °C in 1994. The maximum intensity shown in figure 1(b) mostly occurred on 1 August. During this time, the entire Korean Peninsula was under the influence of a high-pressure system, resulting in low wind speeds and strong solar radiation. Relatively high values were observed, particularly in inland areas. This suggests that even under the influence of the same weather system, the intensity of the heatwave can vary due to factors such as topography, surface conditions, land-sea breeze circulation, and urbanization. Figure 1(c) shows the longest consecutive HWDs, which shows a maximum of 36 d out of 62 d at Gwangju station, while the maximum is 24 d in Jeongup in 1994. This suggests that the heatwave in South Korea in 2018 is unprecedented in magnitude and duration. Notably, the average daily maximum temperature in 2018 is lower than that in 1994, indicating a nonlinear relationship between the seasonal mean temperature and heatwave intensity and duration (Min et al 2020). Meanwhile, the total number of HWDs during the summer shown in figure 1(c) was relatively higher in the western part of South Korea,

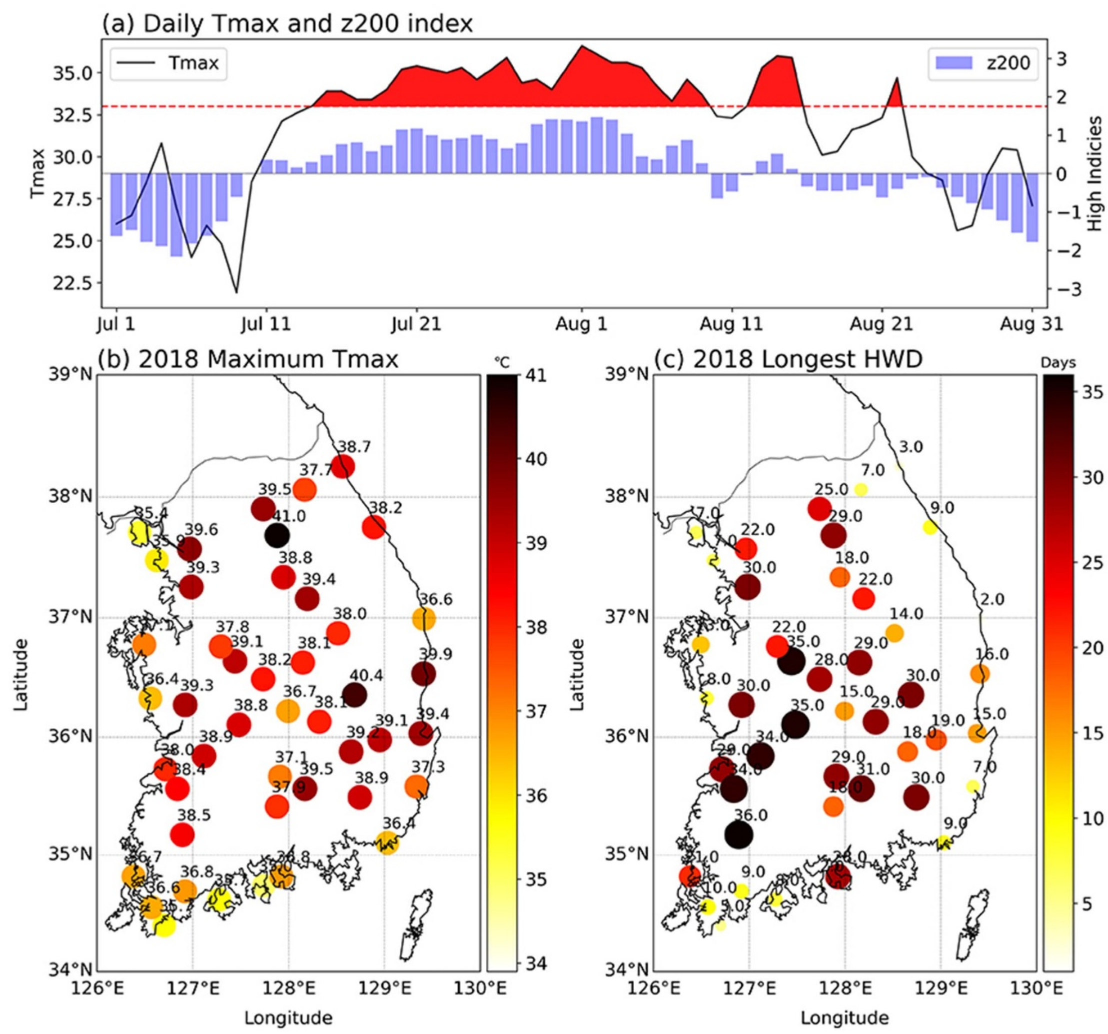

Figure 1. (a) Black solid line indicates daily maximum temperature in the period, dashed red line indicates 33 °C that is the criteria of heatwave, dashed black line indicates averaged climatology value calculated by 5 d running mean. Blue bars indicate 200 hPa geopotential height index calculated in the area above the Korean Peninsula (b) Maximum value of the daily maximum temperature (Tmax) (c) Longest value of the heatwave days in 2018 by each 45 stations.

but this distribution varies each year depending on the influence of the prevailing weather systems.

Figure 1(a) also indicates that the calculated z200 high index using the 200 hPa geopotential height anomalies of the Korean region (35°–45° N, 115°–140° E) is significantly correlated with the daily maximum temperature (r = 0.74). The z500 high index also shows a significant correlation (r = 0.66). Therefore, upper-level anomalous anticyclonic pressure over Korea is strongly related to the Korean heatwave in 2018.

During the heatwave period, a high-pressure system occupies the upper level over South Korea, presumably driven by large-scale atmospheric teleconnections (figure 2). Figure 2 shows atmospheric circulation anomalies during the high summer (JA) of 2018. At the upper-level, Rossby waves propagating in the zonal direction with zonal wavenumbers 5–6 stand out along the mid-latitudes, and one of the centers is located over the Korean Peninsula. This resembles the CGT pattern, as indicated by the high spatial pattern correlation (r = 0.57) over Eurasia (figure 2(b)). In addition, another meridionally-propagating Rossby wave emanates from the Tropics with strong convection over the South China Sea and subsidence over Korea (figure 2(c)), known as the PJ pattern. The pattern correlation between the canonical PJ pattern and the 850 hPa relative vorticity anomalies in 2018 is 0.82 (figure 2(d)). There are also clear negative SLP anomalies over the Arctic with annular positive anomalies in the sub-Arctic (figure 2(e)), which resemble the AO pattern (figure 2(f)), showing a significant pattern correlation (r = 0.48).

Figure 3 shows the time series of CGT, PJ, AO indices, and HWDs, respectively. It is noticeable that all indices of the three known teleconnection indices exhibit a strong positive phase in 2018. In particular, the AO and PJ indices exceed two standard deviation (STD) and one STD, respectively, which are the

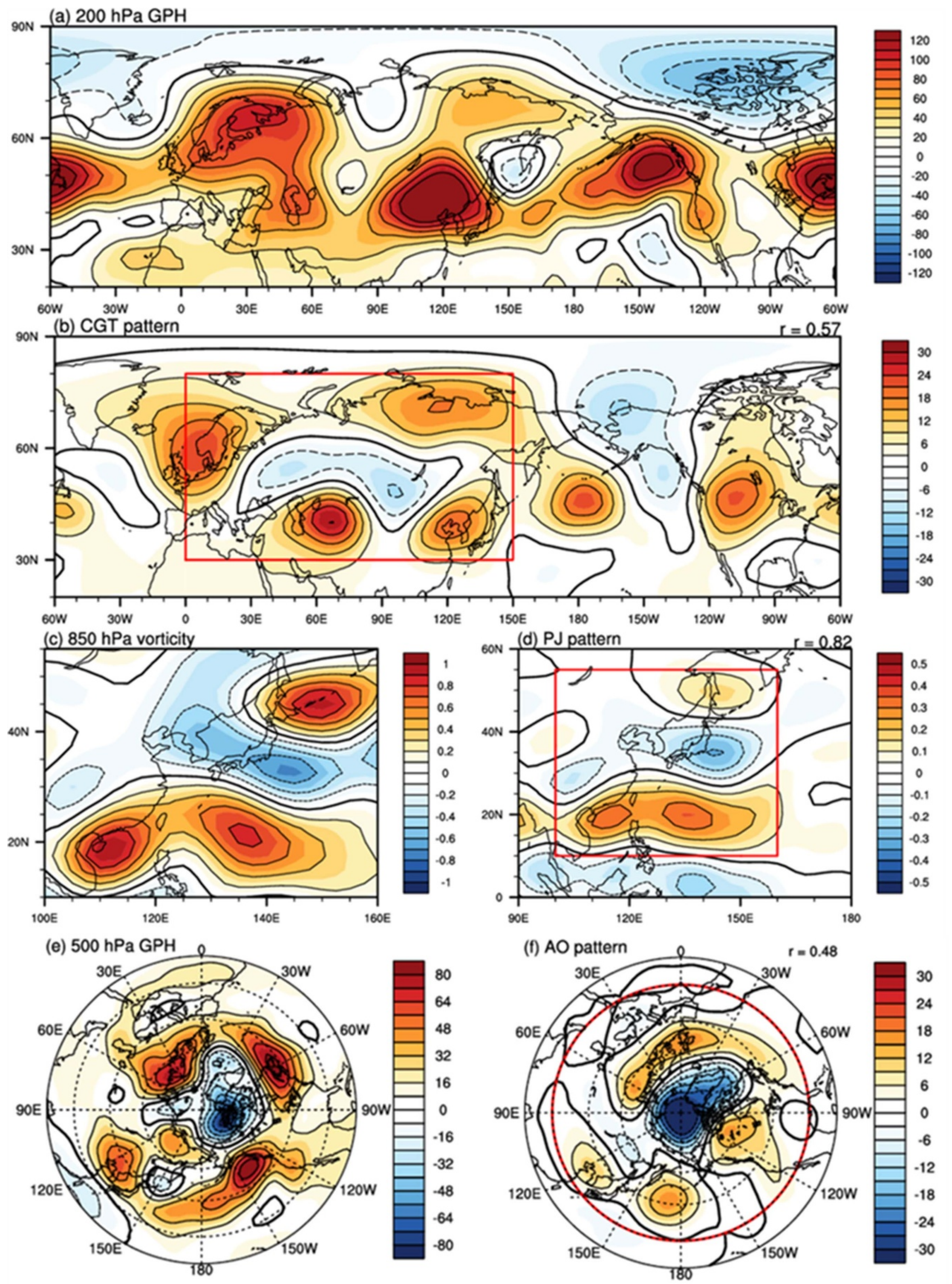

Figure 2. Anomaly of (a) 200 hPa GPH (c) 850 hPa vorticity 500 hPa GPH in 2018 summer (JA mean). Spatial pattern of (b) circum-global teleconnection (CGT), (d) Pacific–Japan (PJ), and (f) Arctic Oscillation (AO). Red box is area used for calculating pattern correlation to anomaly of 2018 case. Pattern correlation is shown in upper right.

highest during the entire analysis period. The CGT index also exceeds one STD, showing the highest value in the recent 20 years. All indices do not show a trend with statistical significance due to large interannual variability (figure 3). It is highly exceptional for three indices to exceed the 1 STD level, and even when extending the analysis period back to 1948, 1994 and 2018 are the only instances (supplementary figure 3). In contrast, three atmospheric teleconnection indices show clear negative phases in 1993, the lowest record of heatwave with 0.1 d.

The relationship between these patterns and heatwaves in Korea has been discussed in previous studies. Kim *et al* (2019) suggested that the upper-level high

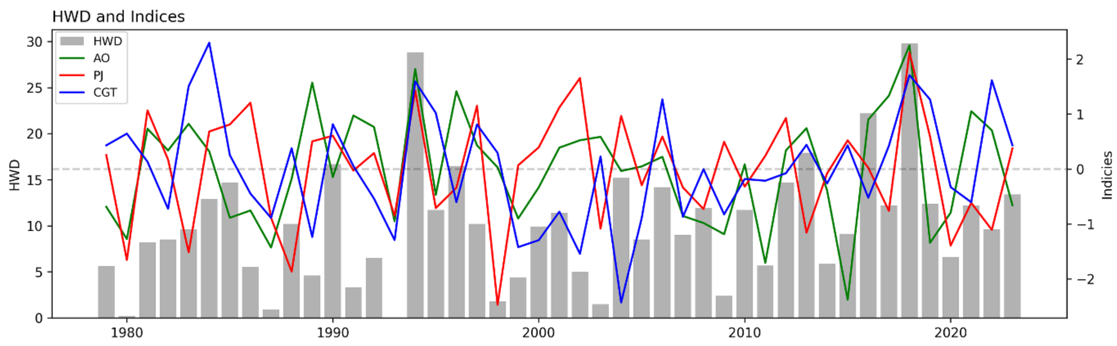

Figure 3. Time series for normalized PJ index (red), CGT index (blue), AO index (green) and HWD (grey bar) during 1979–2023. The left axis is about HWD and the right axis is about pattern indices.

pressure over the Korean Peninsula induced by the zonal CGT-like wave train pattern could be the main cause of the Korean heatwave. Lee and Lee (2016) revealed that convection according to the WNP monsoon variability induced a heatwave over Korea via the PJ pattern. They also suggested that the influence of the AO on the Korean heatwave development showed a pronounced decadal variability and it showed a higher correlation with the Korean heatwave in recent decades since the mid-1990s. This implies that the strong positive AO in 2018 could be one of the major drivers for extreme heatwave events in Korea.

3.2. Effects of CGT, PJ, and AO in Korean HWDs

Three patterns of PJ, CGT, and AO are projected strongly in the observed large-scale circulation patterns in the summer of 2018 that contribute to the strong development of the upper-level high-pressure anomalies in Korea and the prolonged heatwave event. This section examines the extent to which these three patterns account for the interannual variability of HWDs in South Korea using MLR analysis. In addition, this study explores whether the linear combination of the three teleconnection indices can be used as heatwave predictors.

Preceding the MLR analysis, this study examines the statistical independence among the indices. Table 1 shows the correlation coefficients between the teleconnection indices and HWDs. All three indices are highly correlated with the observed HWDs at the 1% significance level. In the meantime, each index shows a low correlation with the other, confirming that all three modes are statistically independent. HWDs also exhibit a statistically significant correlation with the AO, PJ, and CGT indices, as apparent from the MLR by discarding one variable among the three (supplementary table 1).

Table 2 presents the coefficients of the MLR, trend, and time mean. HWD has an increasing trend of one day per year, and the average annual value of HWD is 10.07 d. All indices have significance at the 1% significance level by the Student's t-test. Each

Table 1. Correlation coefficients from linear regression method between each index and HWD. Asterisk (*) indicates significant at the 1% significance level.

	PJ	CGT	AO
PJ	1	−0.04	0.17
CGT	−0.04	1	0.18
AO	0.17	0.18	1
HWD	0.42*	0.39*	0.50*

Table 2. Multiple linear regression coefficients for each index. The increasing trend and time mean are also indicated. The values statistically significant at the 99% confidence level are indicated with asterisk (*).

PJ (day)	CGT (day)	AO (day)	Trend (day yr^{-1})	Mean (day)
2.42*	2.22*	2.43*	1.00*	10.07*

coefficient indicates the change in HWD when each index is increased by 1 STD. The coefficients for PJ, CGT, and AO are 2.42, 2.22, and 2.43, indicating that they have a comparable influence on HWD. These results remain consistent when using different reanalysis datasets (e.g. ERA5; supplementary figure 4).

Figure 4 shows the reconstructed time series of HWD by MLR using the three indices, which shows a high correlation with the observed HWDs ($r = 0.75$, R-squared of 0.56, and adjusted R-squared of 0.51). This suggests that the three dominant atmospheric teleconnection patterns can account for approximately 51% of the interannual variability in HWDs in South Korea. When conducting a leave-one-out cross-validation, the correlation remains as high as $r = 0.66$, indicating that the three teleconnection indices can be used as heatwave predictors.

The contributions of individual teleconnection patterns in the 2018 heatwave case are estimated by multiplying the regression coefficient by each pattern index observed in 2018 (table 3). The total number of HWDs in 2018 is 29.8 d, which is 19.7 d longer than the climatological average of 10.1 d. Global warming, as estimated by the linear trend of the HWDs

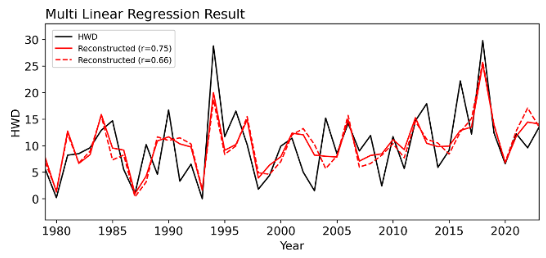

Figure 4. Time series for HWD (black), reconstructed HWD from multiple linear regression (red solid) and forecasting from leave-one-out cross-validation (red dashed). Reconstructed HWD and cross validation results have 95% confidence level.

Table 3. Contribution of each pattern index and trend on observed HWD (31.5 d) in 2018. Bold texts emphasize the contribution of pattern indices.

HWD	CGT	PJ	AO	Climatology	Trend	Residual
29.8	**3.1**	**5.1**	**5.5**	10.1	2.5	2.8

time series, has contributed to an increase of 2.5 d in HWDs compared to the 1970s. The heatwave caused by PJ, CGT, and AO are 5.1, 3.1, and 5.5 d, respectively, showing the most dominant contribution by AO. The remaining 2.8 d of HWDs cannot be accounted for by the MLR analysis, representing a relatively small portion of the total HWDs in 2018. The positive deviation in HWDs due to the three patterns combined is 13.7 d, and this increases to 16.2 d when including the linear trend of 2.5 d. This explains approximately 88.3% of the total HWD anomaly (19.7 d) observed in 2018.

The examination of individual years shows somewhat interesting differences from the 2018 case. For the 1994 case, the second-most HWDs, 20.5 d of the total 28.8 d can be restored by the three atmospheric patterns. For the 2016 case, because the PJ and CGT patterns are negative, they contribute 1.1 d less than the climatology (supplementary table 2). This suggests that the Korean heatwave can be affected by other factors than the three atmospheric teleconnection patterns. As an example, previous studies have indicated the critical role of the Kamchatka blocking (Yoon *et al* 2020) and dry Eurasian soil moisture conditions (Seo *et al* 2020) in the 2016 heatwave event. On the other hand, in the case of the 2018 heatwave, the three patterns are clearly visible in the upper-level large-scale atmospheric fields that contribute to the record-breaking extension of the heatwave.

This study particularly highlights the critical role of upper-level high-pressure anomalies, induced by three teleconnection patterns, in driving prolonged heatwaves in South Korea. The July–August (JA) averaged z200 high-pressure index over the Korean region (35°–45° N, 115°–140° E) shows statistically significant temporal correlations with the three teleconnection indices at the interannual timescale (AO: 0.40, CGT: 0.37, PJ: 0.35) at the 5% significance level, suggesting that all three patterns can significantly influence the formation of the upper-level high-pressure system over the Korean Peninsula. As the number of individual indices showing positive deviations increases, the magnitude of upper-level high-pressure anomalies also increases systematically (supplementary figure 5). A bootstrap test was conducted to test whether this conclusion could vary depending on the sample size. When all three indices are in a strong positive phase, the upper-level high-pressure anomalies produced are much stronger than when influenced by individual indices or two indices combined (supplementary figure 6).

Next, this study investigates the physical mechanisms by which the upper-level high-pressure system induces heatwaves using a heat budget analysis focused on the 2018 case. The analysis reveals that during the heatwave period, the net temperature tendency term is close to zero, indicating that the other three terms are well balanced (figure 5(a)). The heating caused by vertical motion contributes more than that from horizontal advection, suggesting that subsidence and adiabatic heating play a more significant role in sustaining the heatwave under the influence of the upper-level high-pressure system. Diabatic cooling from longwave radiation offsets the heating generated by both horizontal and vertical motion. In the surface energy budget (figure 5(b)), the upper-level high pressure during the heatwave reduced cloud cover, increasing downward shortwave radiation and raising surface temperatures. This suggests that the three climate variability modes amplified the high-pressure system, intensifying the heatwave through increased shortwave radiation and adiabatic heating.

This study further examines the daily fluctuations of the pattern indices and the daily maximum temperature during the 2018 heatwave period (supplementary figure 7). The heatwave begins with a rapid rise in the daily maximum temperatures after July 10, following an upward trend in all three indices in early July. Throughout the entire heatwave period, the indices consistently maintain positive values, with their daily averages matching the monthly indices (daily averages: AO: 1.75, CGT: 1.24, PJ: 2.77). The sustained positive values of the three indices contribute to the formation and persistence of the high-pressure system.

4. Summary and discussions

This study analyzed the dynamical mechanisms for the record-breaking heatwave events in the Korean Peninsula in 2018, with a specific focus on examining

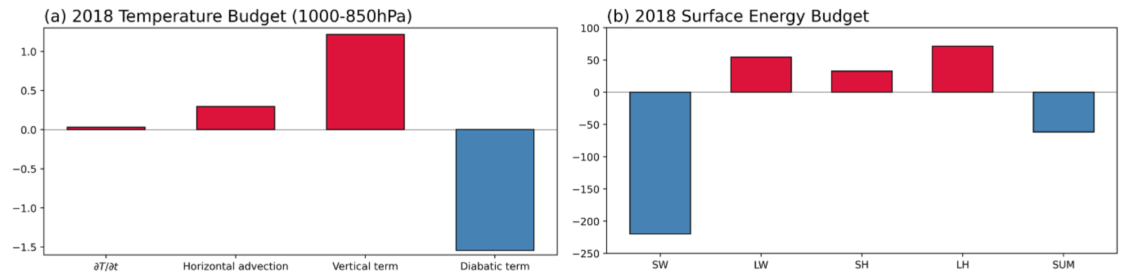

Figure 5. (a) The vertically averaged temperature budget (K d^{-1}) near the Korean Peninsula from 1000 hpa to 500 hpa during the 2018 heatwave period (11 July–14 August). The bars represent air temperature tendency, horizontal advection, vertical motion combining advection and adiabatic heating, and diabatic heating terms. (b) The surface energy budget (W m^{-2}) for net shortwave radiation, net longwave radiation, sensible heat flux, latent heat flux, and sum in the surface. A positive value indicates upward.

the contribution from three dominant atmospheric teleconnection patterns, which were identified as most important in the interannual variability of HWDs based on historical observation data. The multiple linear regression using the indices of the three teleconnection modes fit well with the observed time series of the HWDs. Based on the quantitative analysis, this study indicates that the large-scale teleconnection patterns of PJ, CGT, and AO, which are statistically independent of each other, aggravated the heatwave event in Korea in 2018. In 2018, most of the HWDs can be restored by these three atmospheric patterns.

In this study, we argue that simultaneous development of all three modes is extremely rare based on observational data, potentially leading to an increased frequency of heatwaves. However, since such cases appeared only twice during the historical observation period, further verification is needed. To address this, we examined whether similar compound events occur when using the historical run data from CMIP6 models. The results showed that while simultaneous development of all three modes is highly unusual, these compound events are reproducible in most models, suggesting that increasing the sample size can reveal more occurrences of these rare cases.

As this study estimates global warming contributions based on the linear trend during the short analysis period, changes in heatwave mechanisms due to long-term variability or climate change need to be investigated in a future study. The return period for the 1994 event, as calculated using the GEV distribution (see supplementary figure 1), is 81 years. Nevertheless, a record-breaking number of HWDs occurred just 24 years later in 2018. This indicates that the return period for extreme heatwave events may shorten significantly under the influence of climate change. Furthermore, some of the signals from the three atmospheric patterns are mixed, and their individual roles can not be separated quantitatively using our linear statistical approach. However, this study implies that a dramatic and unprecedented heatwave event could occur if the three patterns develop simultaneously, such as in 1994 and 2018. Ongoing research aims to uncover the dynamical mechanisms through model simulations and forecast experiments. Atmospheric pattern indices such as AO, CGT, and PJ are derived from variables such as SLP, mid-tropospheric geopotential height, and vorticity, and these can be influenced by various slowly-varying boundary conditions like Arctic sea ice, soil moisture, and sea surface temperatures in subseasonal-to-seasonal and interannual timescale. Further research about these relationships needs to be conducted for a more detailed understanding of the teleconnection mechanisms.

A limitation of this study is that the three major teleconnection patterns can explain, at most, approximately 50% of the interannual variability in the number of HWDs on the Korean Peninsula. This suggests that additional predictors could account for the remaining variation. Recently, research on heatwaves has become increasingly active. For example, the relationship with high-latitude Eurasian variability such as the Scandinavia teleconnection pattern (Choi *et al* 2020) has been highlighted. In our analysis, the Scandinavian pattern index shows a statistically insignificant correlation with CGT or AO but exhibits a correlation of approximately 0.4 with PJ, suggesting that part of the heatwave variability in South Korea is linked to both the Eurasian teleconnection and the PJ mode through tropical convection. Zhu *et al* (2020), based on a statistical analysis of heatwaves centered on China, suggest that the dominant mode of interannual variability is related not only to the Eurasian wave train originating from the North Atlantic, but also to the PJ mode, triggered by convective variability over the northwestern Pacific and Maritime Continent. These findings are consistent with the results of this study. As other factors, such as Kamchatka blocking and Eurasian dry soil conditions, are further identified, they could be considered as additional predictors in our linear regression model, potentially improving our ability to make long-range or seasonal predictions.

Data availability statement

The data cannot be made publicly available upon publication because no suitable repository exists for hosting data in this field of study. The data that support the findings of this study are available upon reasonable request from the authors.

Acknowledgments

This study was supported by the Korea Meteorological Administration Research and Development Program under Grant KMI2017-02410 and Korea Environment Industry &Technology Institute(KEITI) through 'Climate Change R&D Project for New Climate Regime.', funded by Korea Ministry of Environment(MOE) (2022003560002).

ORCID iDs

Hyerin Kim https://orcid.org/0009-0002-8623-386X
Nakbin Choi https://orcid.org/0000-0002-8696-5916
Myong-In Lee https://orcid.org/0000-0001-8983-8624
Sunlae Tak https://orcid.org/0009-0009-2423-936X
Dong-Hyun Cha https://orcid.org/0000-0001-5053-6741
Seung-Ki Min https://orcid.org/0000-0002-6749-010X

References

Choi N and Lee M I 2019 Spatial variability and long-term trend in the occurrence frequency of heatwave and tropical night in Korea *Asia-Pac. J. Atmos. Sci.* **55** 101–14

Choi N, Lee M-I, Cha D-H, Lim Y-K and Kim K-M 2020 Decadal changes in the interannual variability of heat waves in East Asia caused by atmospheric teleconnection changes *J. Clim.* **33** 1505–22

Ding Q H and Wang B 2005 Circumglobal teleconnection in the Northern Hemisphere summer *J. Clim.* **18** 3483–505

Ha K-J, Yeo J-H, Seo Y-W, Chung E-S, Moon J-Y, Feng X, Lee Y-W and Ho C-H 2020 What caused the extraordinarily hot 2018 summer in Korea? *J. Meteorol. Soc. Jpn. Ser.* II **98** 153–67

Kalnay E *et al* 1996 The NCEP/NCAR 40 year reanalysis project *Bull. Am. Meteorol. Soc.* **77** 437–71

Kim M-K, Oh J-S, Park C-K, Min S-K, Boo K-O and Kim J-H 2019 Possible impact of the diabatic heating over the Indian subcontinent on heat waves in South Korea *Int. J. Climatol.* **39** 1166–80

Kim Y-H, Min S-K, Stone D A, Shiogama H and Wolski P 2018 Multi-model event attribution of the summer 2013 heat wave in Korea *Weather Clim. Extremes* **20** 33–44

Kosaka Y and Nakamura H 2010 Mechanisms of meridional teleconnection observed between a summer monsoon system and a subtropical anticyclone. Part I: the Pacific–Japan pattern *J. Clim.* **23** 5085–108

Lee W-S and Lee M-I 2016 Interannual variability of heat waves in South Korea and their connection with large-scale atmospheric circulation patterns *Int. J. Climatol.* **36** 4815–30

Min S-K, Kim Y-H, Lee S-M, Sparrow S, Li S, Lott F C and Stott P A 2020 Quantifying human impact on the 2018 summer longest heat wave in South Korea *Bull. Am. Meteorol. Soc.* **101** S103–S108

Min S-K, Kim Y-H, Paik S, Kim M-K and Boo K-O 2015 19. Anthropogenic influence on the 2014 record-hot spring in Korea *Bull. Am. Meteorol. Soc.* **96** S95–S99

Nitta T 1987 Convective activities in the tropical western Pacific and their impact on the Northern Hemisphere summer circulation *J. Meteorol. Soc. Jpn. Ser.* II **65** 373–90

Pachauri R K *et al* 2014 *Climate Change 2014: Synthesis Report. Contribution of Working Groups I, II and III to the Fifth Assessment Report of the Intergovernmental Panel on Climate Change* (IPCC)

Park C-K and Schubert S D 1997 On the nature of the 1994 East Asian summer drought *J. Clim.* **10** 1056–70

Park J and Chae Y 2020 Analysis of heat-related illness and excess mortality by heat waves in South Korea in 2018 *J. Korean Geogr. Soc.* **55** 391–408

Ren L, Zhou T and Zhang W 2020 Attribution of the record-breaking heat event over Northeast Asia in summer 2018: the role of circulation *Environ. Res. Lett.* **15** 054018

Seo E, Lee M, Schubert S D, Koster R D and Kang H 2020 Investigation of the 2016 Eurasia heat wave as an event of the recent warming *Environ. Res. Lett.* **15** 114018

Thompson D W and Wallace J M 1998 The Arctic Oscillation signature in the wintertime geopotential height and temperature fields *Geophys. Res. Lett.* **25** 1297–300

Wilks D S 2011 *Statistical Methods in the Atmospheric Sciences* (Academic)

Yeo S-R, Yeh S-W and Lee W-S 2019 Two types of heat wave in Korea associated with atmospheric circulation pattern *J. Geophys. Res.* **124** 7498–511

Yoon D, Cha D, Lee M, Min K, Kim J, Jun S and Choi Y 2020 Recent changes in heatwave characteristics over Korea *Clim. Dyn.* **55** 1685–96

Zhu B, Sun B and Wang H 2020 Dominant modes of interannual variability of extreme high-temperature events in eastern China during summer and associated mechanisms *Int. J. Climatol.* **40** 841–57